10th International Conference on Composite Science and Technology
ICCST/10
A.L. Araújo, J.R. Correia, C.M. Mota Soares, et al. (Editors)


# LOCKING AND STABILITY OF 3D TEXTILE COMPOSITE REINFORCEMENTS DURING FORMING

**Sylvain Mathieu, Nahiene Hamila, Philippe Boisse***

University of Lyon, INSA-Lyon, LaMCos, F-69621, France
* Corresponding author: Philippe.Boisse@insa-lyon.fr

**Key words:** Composites, Modeling, Experimental validation, Industrial applications.

**Summary:** *Some limits of an hyperelastic constitutive law for 3D textile preforms are analyzed. The model is macroscopic and aims to determine the strains and stresses of the whole 3D preform. The strain energy potential is defined for elementary deformation modes. The dependence of the strain energy potential on the material privileged directions can be introduced explicitly. Structural tensors representative of the anisotropy of the material are introduced. The interlock reinforcement has three privileged directions: the warp direction, the weft direction and a third direction through the preform thickness. The constitutive law has proven to be effective but the finite element formulation into which it is implemented may be spurious in some cases. Enhancements of the numerical approach in order to avoid these problems will be presented*

## 1 INTRODUCTION

The mechanical properties of 3D fabric-reinforced composites are highly specific. Their high rigidity, low density and improved delamination resistance designate them as a first-choice material for state-of-the-art aeronautic parts. These materials are crafted by a 3D weaving process of, predominantly, carbon or ceramic yarns. Some efforts concentrate on simulating the behavior of woven composite reinforcements during the initial phase of the process [1-4]. The final position of the yarns and, consequently, the fiber density are determined during this step. This information is of major importance, as it will affect directly the feasibility and quality of the following injection step. The variation of shear angle between yarns modifies the permeability of the fabric.

Hyperelastic laws has proven to be effective [5-8] but the finite element formulation based on these constitutive laws show some specific numerical problems. On the first hand, limitations in the constitutive law orientation inside the element has been demonstrated. The numerical simulation of bias extension test with standard elements has shown overestimated loads and mispredicted specimen shape when element edges are not oriented properly. This phenomenon is called tension locking [9], or intra-ply shear locking [10,11]. A simple element based on reduced integration plus physical stabilization is proposed. On the other hand, instabilities in bending dominated simulation have been observed which lead to results not seen experimentally. A possible solution to the problem is proposed.

## 2 ANISOTROPIC HYPERELASTIC CONSTITUTIVE EQUATION

The following hyperelastic law is detailed in [12]. Thick interlock reinforcements have three privileged directions: a warp direction $\underline{M}_1$, a weft direction $\underline{M}_2$ and a third direction $\underline{M}_3$ orthogonal to the plane defined by $\underline{M}_1$ and $\underline{M}_2$. The vector $\underline{M}_3$ is oriented through the thickness of the preform but does not correspond to a third yarn direction in the case of interlock fabrics. The following structural tensors are defined for $\underline{M}_i$ vectors [13]:

$$\underline{\underline{M}}_1 = \underline{M}_1 \otimes \underline{M}_1, \quad \underline{\underline{M}}_2 = \underline{M}_2 \otimes \underline{M}_2 \quad \text{and} \quad \underline{\underline{M}}_3 = \underline{M}_3 \otimes \underline{M}_3 \tag{1}$$

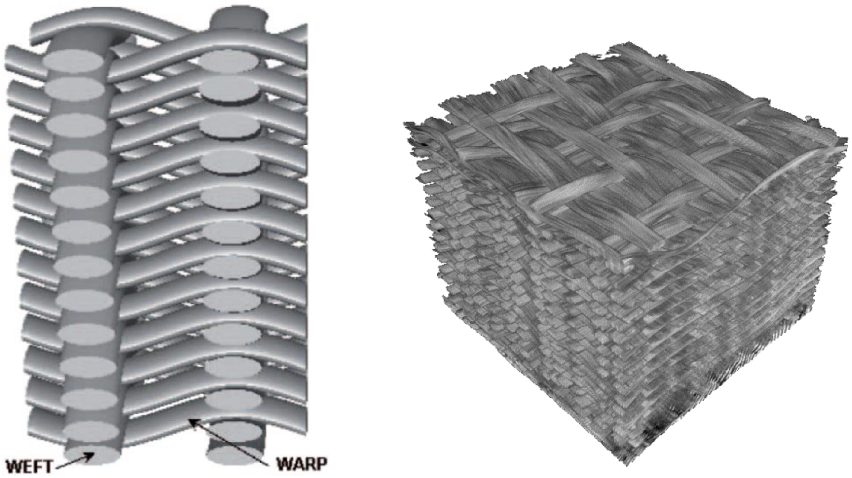


(b)

Figure. 1. Ply to ply interlock.

The representation theorems [18,19] show that, for an orthotropic material, the strain energy density function of a hyperelastic law is in the form:

$$w^{orth} = w^{orth}\left(I_1, I_2, I_3, I_{41}, I_{42}, I_{43}, I_{412}, I_{423}, I_{51}, I_{52}, I_{53}\right) \tag{2}$$

where $I_1, I_2, I_3,$ are the invariants of the right Cauchy-green tensor $\underline{\underline{C}}$ defined by:

$$I_1 = Tr\left(\underline{\underline{C}}\right) \qquad I_2 = \frac{1}{2}\left(Tr\left(\underline{\underline{C}}\right)^2 - Tr\left(\underline{\underline{C}}^2\right)\right) \qquad I_3 = Det\left(\underline{\underline{C}}\right) \tag{3}$$

and:

$$I_{4i} = \underline{\underline{C}} : \underline{\underline{M}}_i = \underline{M}_i \cdot \underline{\underline{C}} \cdot \underline{M}_i, \quad I_{4ij} = \underline{M}_i \cdot \underline{\underline{C}} \cdot \underline{M}_j \quad \text{and} \quad I_{5i} = \underline{\underline{C}}^2 : \underline{\underline{M}}_i = \underline{M}_i \cdot \underline{\underline{C}}^2 \cdot \underline{M}_i \tag{4}$$

are the mixed invariants of the structural tensors where i varies from 1 to 3.
The deformation modes of interlock reinforcements are the deformation modes induced by the thickness of the reinforcement added to those of a 2D woven fabric. Six deformation modes are thus considered: extensions in warp and weft directions, transverse compaction, in-plane shear and transverse shear in warp and weft directions (Fig. 2). For each deformation mode, physical

strain invariants can be defined. They are combinations of the invariants defined in (3) and (4) and are based on physical observations of interlock deformation modes.

$$I^1_{elong} = \frac{1}{2} ln\left(I_{41}\right) \qquad I^2_{elong} = \frac{1}{2} ln\left(I_{42}\right) \qquad I_{comp} = \frac{1}{2} \ln\left(\frac{I_3}{I_{41} I_{42}\left(1 - I^2_{cp}\right)}\right) \tag{5}$$

$$I_{cp} = \frac{I_{412}}{\sqrt{I_{41} I_{42}}} = sin\left(\gamma\right) \qquad I_{ct1} = \frac{I_{413}}{\sqrt{I_{41} I_{43}}} = sin\left(\alpha_{13}\right) \qquad I_{ct2} = \frac{I_{423}}{\sqrt{I_{42} I_{43}}} = sin\left(\alpha_{23}\right) \tag{6}$$

It is assumed that the contribution of each deformation mode is independent from the others. As a result the strain energy density is the sum of the different strain energies:

$$w = w^1_{elong}\left(I^1_{elong}\right) + w^2_{elong}\left(I^2_{elong}\right) + w_{comp}\left(I_{comp}\right) + w_{cp}\left(I_{cp}\right) + w_{ct1}\left(I_{ct1}\right) + w_{ct2}\left(I_{ct2}\right) \tag{7}$$

The second Piola-Kirchhoff stress tensor $S$ is obtained by differentiation of $w$, using the fact that each contribution is independent from one another:

$$\underline{\underline{S}} = 2\frac{\partial w}{\partial \underline{\underline{C}}} = 2\frac{\partial w}{\partial I_k}\frac{\partial I_k}{\partial \underline{\underline{C}}} = 2\frac{\partial w_k}{\partial I_k}\frac{\partial I_k}{\partial \underline{\underline{C}}} \tag{8}$$

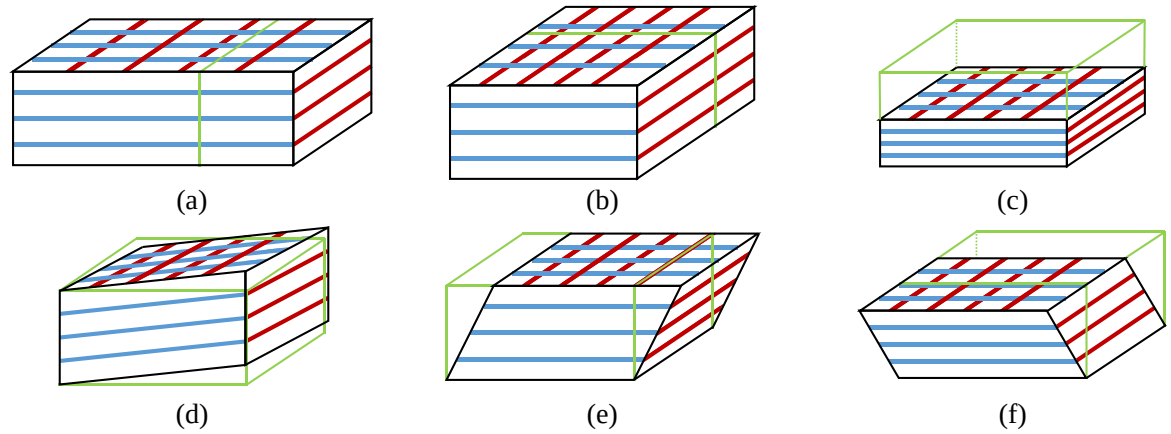


Figure 2. Deformation modes of interlock reinforcements (a and b) stretches, (c) transverse compression, (d) in-plane shear and (e and f) transverse shears.

The form of each strain energy density of equation (7) is chosen as universal as possible to be relevant for any material:

$$w = \begin{cases} k_1 I^2 + k_2 I^3 + k_3 I^4 + k_4 I^5 + k_5 I^6 + k_6 I^7 & \text{if } I > 0 \\ k_1 I^2 + k_7 I^3 + k_8 I^4 + k_9 I^5 + k_{10} I^6 + k_{11} I^7 & \text{if } I \le 0 \end{cases} \tag{9}$$

where $k_i$ are material parameters, and $I$ the physical invariant related to the specific strain energy $w$. The coefficients are identified by simple tests: tensile tests in the warp and weft directions, compaction test, bias extension test (in-plane shear), and simple transverse shear

tests. The identification is simplified by the uncoupling assumption: each experimental test is only contributing to one specific strain energy density. For more information, a complete identification of the six strain energy densities and the validation on different simple cases are detailed in [12].

## 3 TENSION LOCKING

The simulation of a bias extension test highlights a specific numerical locking that can occur for textile reinforcements. The fibers are oriented at ±45°. The simplest mesh is obtained with a regular division in rectangular elements. In this case, the fibres are not aligned with the elements. A standard finite element analysis leads to loads on the tensile machine far larger than those measured experimentally (Fig. 3). The final shape of the specimen is also wrong (Fig. 2)

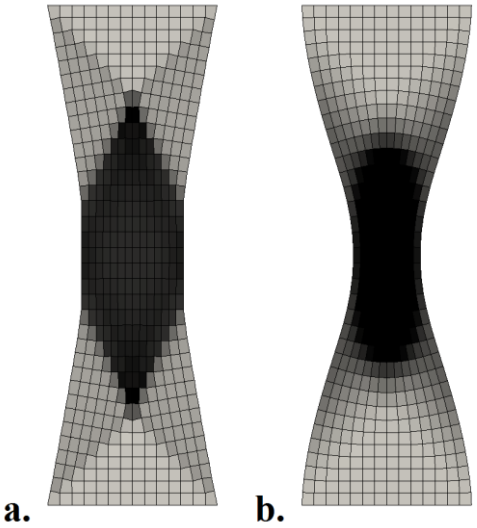


Figure 2: Bias extension test specimen final shape simulation meshed regularly with (a.) reduced integration with specific hourglass stabilization and (b.) full integration elements

The use of one point quadrature quadrilateral elements is a possible solution to this locking phenomenon. In order to avoid spurious singular modes, a specific stabilization procedure is proposed. It is based on a γ-projection method. It only acts on the non-constant part of the in-plane shear strains. Based on the underintegrated element, this approach is numerically efficient. It is shown that locking is eliminated (Fig. 4). Details on the specific stabilization procedure are given in [9].

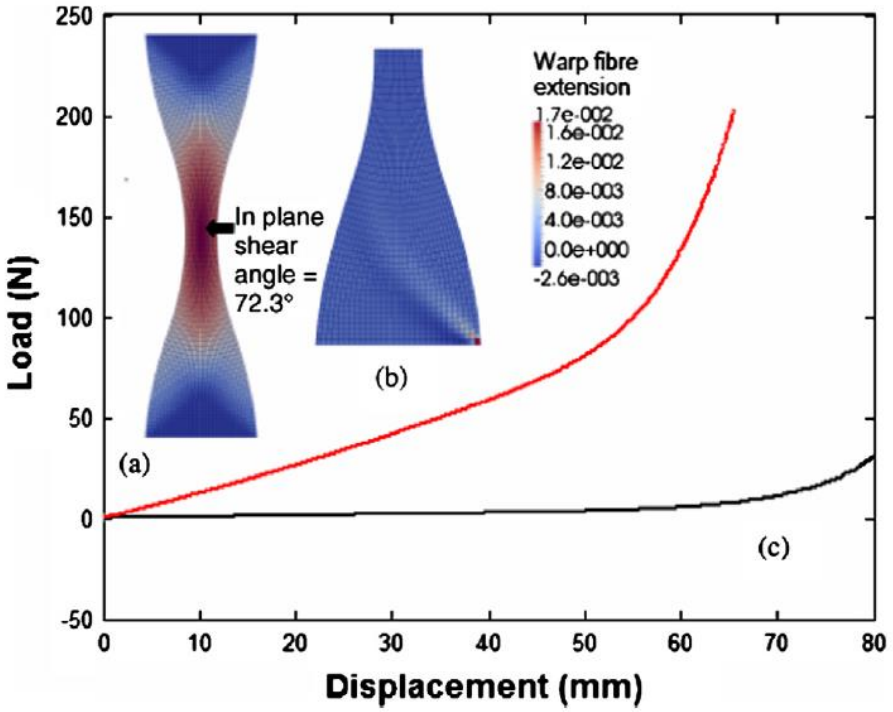


Figure 3: Mesh aligned with the specimen, unaligned with fibres.
Comparison of the load-displacement curve from experiments (black) and simulation (red).

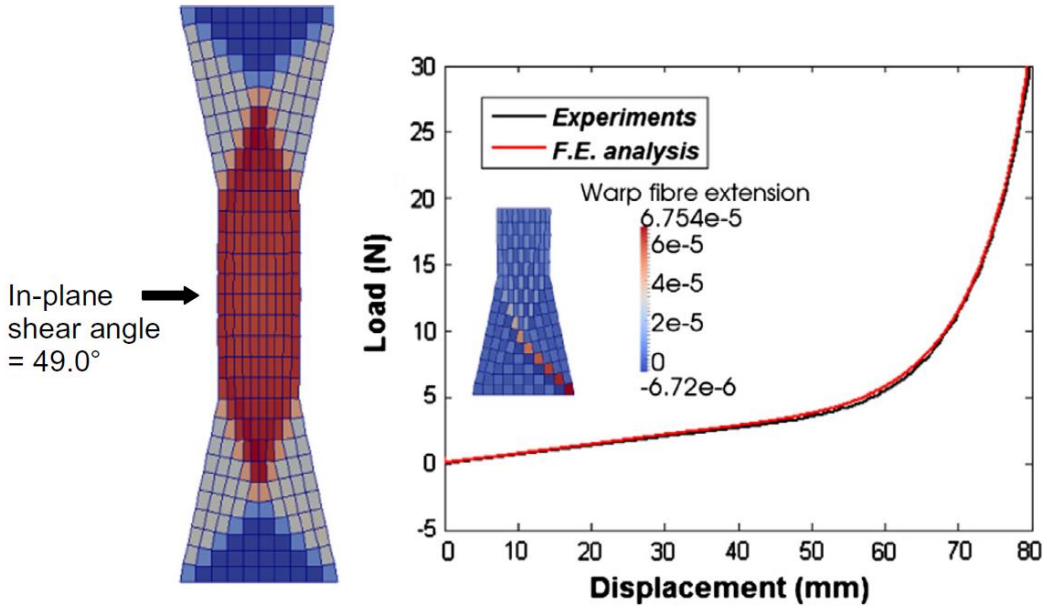


Figure 4: Mesh unaligned with fibres. Simulation using an underintegration and a specific stabilization.
Comparison of the load-displacement curve from experiments (black) and simulation (red).

## 4 FLEXURAL PARASITIC MODES

A second difficulty is highlighted in 3D reinforcement deformation simulations. A three point bending force is applied to an interlock specimen. Figure 5 shows the deformed shape for a 40mm displacement of the central point. Because of the large tensile stiffness of the

yarns, the deformation of the specimen is mainly due to transverse shear. The results of the simulations are incoherent with the experiment and show spurious peaks. Those are the result of the emergence of parasitic patterns due to the high anisotropy of dry thick woven preforms. Two solutions have been developed in [14] in order to avoid this spurious modes. One is based on the so called Fbar method [15] and the other one introduce a local stiffness of fibres in the finite element computation. The curvatures of the fibres are computed using a scheme used in rotation free shell elements [16, 17]. As it is shown in Fig. 5, the spurious bending modes are avoid. More details on the approaches are given in [18, 19]

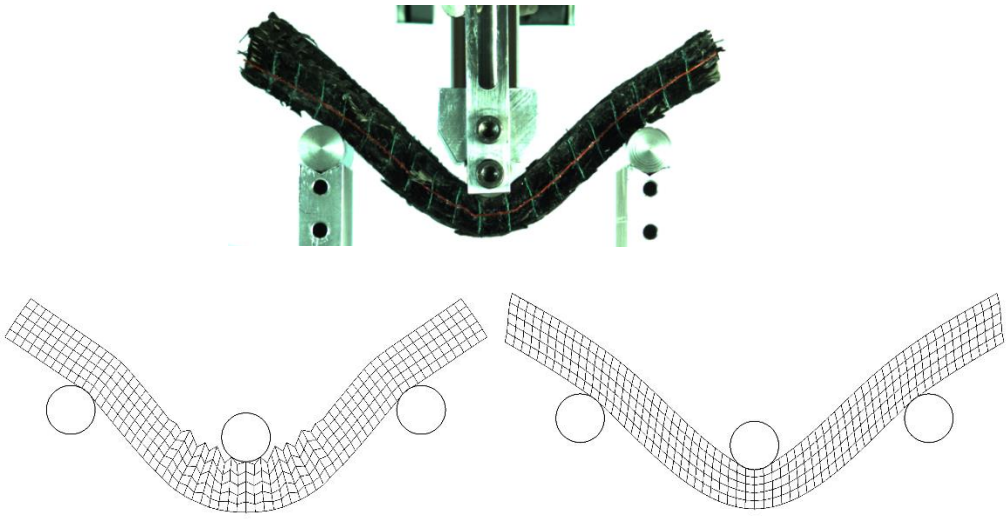

Figure 5: Three point bending. Emergence of spurious transverse modes and correction taking into account local bending stiffness.

## 4 CONCLUSIONS

The extension of the simulation of composite forming to the three-dimensional case of thick woven reinforcements bring to light new modeling challenges. The highly anisotropic material behavior induces, among other phenomena, tension locking and the development of spurious transverse modes in bending-dominated simulations. Solutions have been proposed to these difficulties in the present work.

## REFERENCES

1. De Luca P, Pickett AK. Numerical and experimental investigation of some press forming parameters of two fibre reinforced thermoplastics: APC2-AS4 and PEICETEX. Compos Part A, 29:101–10, 1998
2. Hsiao SW, Kikuchi N. Numerical analysis and optimal design of composite thermoforming process. Comput Method Appl Mech Eng. 177:1–34, 1999
3. Zouari B, Daniel J.L, Boisse B. A woven reinforcement forming simulation method. Influence of the shear stiffness Computers and structures 84 (5): 351-363, 2006

4. Boisse P. Finite element analysis of composite forming. In: Long AC, editor. Composite forming technologies. Woodhead Publishing Limited; 2007.
5. Spencer, A.J.M. Continuum Theory of the Mechanics of Fibres-reinforced Composites, Springer-Verlag, New York.Springer-Verlag, New York, 1984
6. Holzapfel, G.A., Gasser, T.C. and Ogden, R.W. A New Constitutive Framework for Arterial Wall Mechanics and Comparative Study of Material Models, Journal of Elasticity, 61: 1-48, 2000
7. A. Charmetant, J. G. Orliac, E. Vidal-Sallé, P. Boisse, Hyperelastic model for large deformation analyses of 3D interlock composite preforms, Compos Sci Technol, 72, 1352‑1360, 2012
8. J. Pazmino, S.Mathieu, V. Carvelli, P. Boisse, S. V. Lomov, Numerical modelling of forming of a non-crimp 3d orthogonal weave e-glass composite reinforcement, Composites: Part A 72, 207–218, 2015
9. N. Hamila, P. Boisse, Locking in simulation of composite reinforcement deformations. Analysis and treatment, Compos. Part A, 53,109‑117, 2013
10. X. Yu, B. Cartwright, D. McGuckin, L. Ye, Y.-W. Mai, Intra-Ply shear locking in finite element analyses of woven fabric forming processes, Compos. Part A, 37: 790-803, 2006
11. R. H. W. ten Thije, R. Akkerman, Solutions to intra-ply shear locking in finite element analyses of fibre reinforced materials, Compos. Part A, 39 : 1167‑1176, 2008
12. A. Charmetant, J. G. Orliac, E. Vidal-Sallé, et P. Boisse, « Hyperelastic model for large deformation analyses of 3D interlock composite preforms », Compos Sci Technol, vol. 72, p. 1352‑1360, 2012.
13. J. P. Boehler, "Lois de comportement anisotrope des milieux continus," J. Mécanique vol. 17, pp. 153–70, 1978.
14. S. Mathieu, N. Hamila, F. Dupé, C. Descamps, P. Boisse, Solutions to spurious transverse modes in 3D composite reinforcement simulation, Int. J. Solids and Structures, 2015, submitted.
15. J. C. Simo, R. L. Taylor, et K. S. Pister, « Variational and projection methods for the volume constraint in finite deformation elasto-plasticity », Comput Meth Appl Mech Eng, 51: 177‑208, 1985
16. E. Onate et M. Cervera, « Derivation of thin plate bending element with one degree of freedom per node : a simple three node triangle », Eng. Comput., 10: 543‑561, 1993
17. F. Sabourin et M. Brunet, « Analyses of plates and shells with a simplified 3 node triangular element », Thin Walled Struct., 21: 238‑251, 1995
18. S. Mathieu, « Mechanical behavior modeling of CMC interlocks through the forming and pyrolysis proceses », Ph.D. these INSA Lyon, 2014
19. S. Mathieu, N. Hamila, F. Bouillon, P. Boisse, Enhanced modeling of 3D composite preform deformations taking into account local fiber bending stiffness, Compos Sci Technol, Submitted.